Persistent Spin Helix-based Spin Field Effect Transistor

Zhizhong Chen[1], Jian Shi[1]
[1]Rensselaer Polytechnic Institute, Troy, New York, USA, shij4@rpi.edu

Abstract

Spintronic device is promising due to their potential merits of low power consumption and fast operation. In this work, we present the effect of persistent spin helix, barrier resistance, spin polarization and channel resistance on the magnetoresistance of spin field effect transistor (FET) when the channel material carries strong spin-orbit coupling (SOC) and persistent spin helix (PSH). Our device shows promising spintronic performance with current device technologies.
(Keywords: persistent spin helix, Rashba and spin)

Introduction

In 2000, it was theoretically formulated that the spin injection efficiency between a ferromagnet (FM) and a semiconductor (SC) was lower than 1% with some simulation data received from experimental results in or before 2000.[1] This low spin injection efficiency was attributed to the conductivity mismatch between FM and semiconductor layer.[1,2] It was later demonstrated that the spin injection efficiency could be significantly boosted by introducing a barrier at the interface, either a Schottky barrier or a tunneling barrier, so as to resolve the conductivity mismatch issue.[2,3] By merit of this additional barrier layer, high spin injection efficiency >50% were demonstrated using various native Schottky barrier[4,5] or extrinsically grown oxide tunneling barriers (e.g. MgO)[6]. With the spin injection issue addressed, one limiting factor for spin FET performance instead became the severe loss of spin population or coherence in the channel material.[7,8] It is believed that the use of high electric fields and high doping concentration in semiconducting channel materials will accelerate the spin decoherence.[7] With these understandings and further engineering, the performance of spin FET showed remarkable progress in past 5 years. For example, in 2015, nearly 100% spin injection efficiency and all-semiconductor all-electrical operation were achieved in a Si spin-FET.[9] In 2017, by combining the strong SOC of MoS_2 and long spin diffusion length in graphene, the room-temperature spin FET was demonstrated in a MoS_2/graphene heterostructure.[10]

Under this context, the uniqueness of the symmetry-protected spin manipulation (i.e. PSH) becomes obvious.[11] The strong-SOC based spin FET features the short spin precession length λ_{PSH} that enables the device miniaturization (Si-based spintronic device has a miniaturization issue due to the weak SOC). Together with PSH, strongly controllable and coherent spin precession become possible.

In this work, we simulate the spintronic device performance based on SC materials that hold strong SOC and PSH. Exemplified materials include monochalcogenides and Bi-based oxides.[12,13] Based on the model developed by Fert and Jaffres[14], we here quantify the role of channel resistance, spin injection efficiency etc. on the potential of device performance, especially the projected magnetoresistance.

Results and Discussions

This model is based on a FM-SC-FM structure with two tunneling barriers between (Fig. 1). The length of the two FM electrodes are assumed to be semi-infinite, while a finite nonmagnetic SC layer (carrying strong SOC and PSH) is given a thickness t_N. The resistivity of FM and semiconductor are ρ_F and ρ_N, respectively. The spin diffusion length of FM and semiconductor are λ_F and λ_N, respectively. λ_N is approximated as the spin precession length since a PSH structure is assumed. The interfacial resistance of tunnel barrier is given by r_b with unit $\Omega \cdot m^2$. In most evaluations, the spin injection-associated coefficient γ will be treated as 0.5 and β as 0.46 which is for typical FM material Co[14]. These are experimentally practical values[14]. In addition, r_N and r_F stand for the product of resistivity and spin

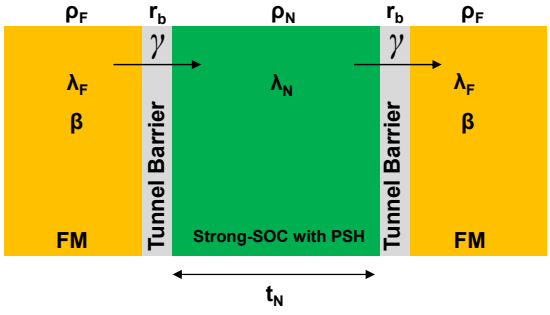

Fig. 1. The structure of the modeled device, with two FM electrodes, one semiconducting channel and two tunneling barriers between.

diffusion length in semiconductor and FM, respectively. The magnetoresistance ΔR, which is the difference in the resistance under the parallel/antiparallel configurations can be calculated below[14]:

$$\Delta R = \frac{2(\beta r_F + \gamma r_b)^2}{(r_b + r_F)\cosh\left(\frac{t_N}{\lambda_N}\right) + \frac{r_N}{2}\left(1 + \left(\frac{r_b}{r_N}\right)^2\right)\sinh\left(\frac{t_N}{\lambda_N}\right)}$$

The resistance with parallel magnetization in the FM electrodes can be calculated by:

$$R_P = 2(1-\beta^2)r_F + \frac{r_N t_N}{\lambda_N} + 2(1-\gamma^2)r_b + 2\frac{(\beta-\gamma)^2 r_F r_b + r_N(\beta^2 r_F + \gamma^2 r_b)\tanh\left(\frac{t_N}{2\lambda_N}\right)}{r_F + r_b + r_N \tanh\left(\frac{t_N}{2\lambda_N}\right)}$$

If this magnetoresistance is normalized by the resistance under parallel configuration, a unitless relative ratio $\Delta R/R_P$ can be calculated. Using this model, Fert et al assumed two Co electrodes and demonstrated the effect of interface barrier resistance r_b and semiconductor thickness on $\Delta R/R$. They showed that the maximum $\Delta R/R_P$ around 0.33 was achieved when r_b is around 10^{-8} Ω•m^2 and t_N = 20 nm.[14]

In our case, without losing generality, we inherit the parameters for Co electrodes, namely $\beta = 0.46$, λ_F = 60 nm, $r_F = 4.5\times10^{-15}$ Ω•m^2. In Fig. 2 and 3 we systematically show the analysis of the roles of r_b, γ, ρ_N and λ_N (or the spin precession length therein) on $\Delta R/R_P$. Since in our design the channel length is supposed to match the spin precession length, we always assume $\lambda_N = t_N$ except in Fig. 3b. We also assume γ to be 0.5 (except in Fig. 2b) since this value is rather approachable with state-of-the-art spin injection techniques. The channel resistivity ρ_N = 0.1 Ω•m can be engineered with chemical doping.

We first show the improvement of magnetoresistance after the insertion of tunneling barriers. Fig. 2a shows that a maximum $\Delta R/R_P$ around 0.08 can be expected when r_b ranges around 10^{-8} Ω•m^2, which is highly consistent with the findings of Fert et al. After switching the semiconductor thickness among 20, 50 and 100 nm, r_b that renders a peak $\Delta R/R_P$ slightly varied while the maximum $\Delta R/R_P$ stayed basically unaltered. The rapid decrease of $\Delta R/R_P$ when r_b is deviated from 10^{-8} Ω•m^2 indicates

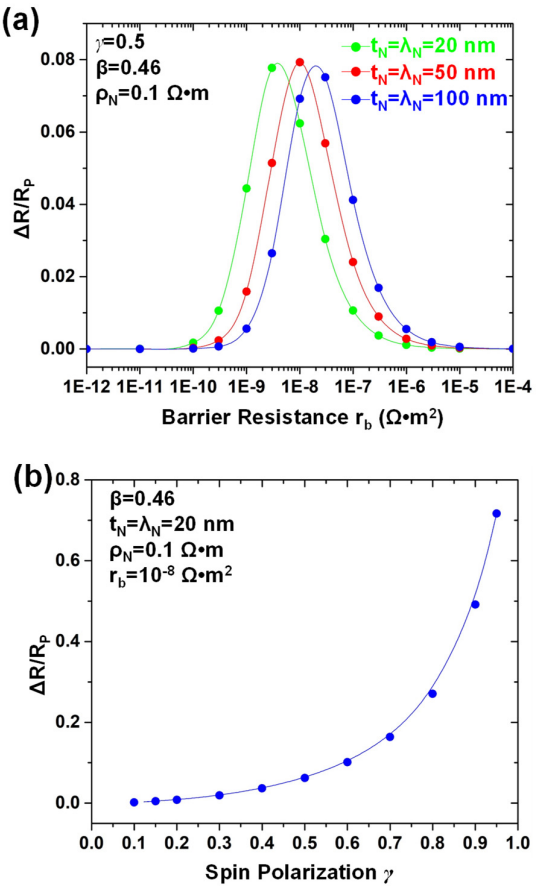

Fig. 2. The normalized magnetoresistance under (a) different barrier resistances, (b) different spin polarizations.

the effectiveness of tunneling barrier in improving spin injection efficiency.

Fig. 2b shows the effect of γ on $\Delta R/R_P$. A superlinear increase in $\Delta R/R_P$ is observed. It should be noted that $\Delta R/R_P$ improves significantly if γ exceeds 0.6. The effect of channel resistivity ρ_N is calculated in Fig. 3a. A maximum $\Delta R/R_P$ is reached when ρ_N = ~0.3 Ω•m.

The role of spin diffusion length (or equivalently the spin precession length) in the channel is analyzed in Fig. 3b. It should be noted that here the channel length t_N is fixed as 20 nm, while λ_N is changed independently. The fact that $\Delta R/R_P$ becomes negligible when λ_N is smaller than 5 nm can be understood as the complete spin randomization induced by strong spin precession. On the other hand, that $\Delta R/R_P$ saturates around 0.26 when λ_N exceeds around 200 nm indicates a rather tiny loss of spin

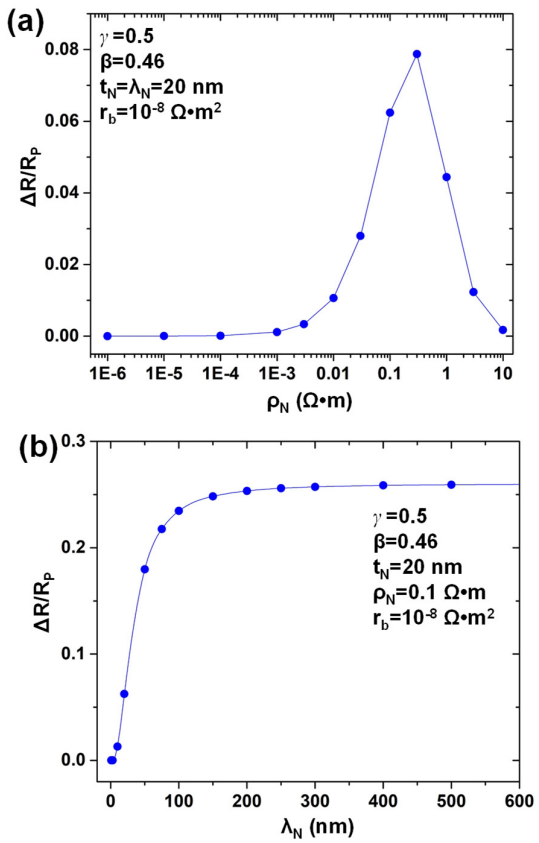

Fig. 3. The normalized magnetoresistance under (a) different channel resistivity and (b) different spin diffusion length in channel.

coherence.

Overall, the comparisons in Figs. 2 and 3 indicate that, assuming a decent γ of 0.5, the introduction of tunneling barriers into the spin FET will enhance device performance such that around 8% magnetoresistance is expected. If γ can be further improved, the device performance would improve even more (e.g. when γ = 0.9, magnetoresistance is 50%).

Conclusion and Perspective

The potential of our PSH-based spin FET can be understood from the following aspects: (1) the PSH guarantees more tolerance to near-ambient operation temperature (300 K) since no ballistic operation is required; (2) The strong SOC allows a shorter channel, and in turn reduces channel resistance and improves overall device performance. The estimated 8% magnetoresistance change could be further improved with advanced spin injection techniques and optimized tunneling barriers.

Acknowledgments

The authors gratefully acknowledge the support from US NSF under award no. 2031692.

References

1. Schmidt, G., Ferrand, D., Molenkamp, L., Filip, A. & Van Wees, B. Physical Review B 62, R4790, (2000).
2. Albrecht, J. & Smith, D. Physical Review B 66, 113303, (2002).
3. Dankert, A., Dulal, R. S. & Dash, S. P. Scientific reports 3, 3196, (2013).
4. Huang, L. et al. Applied Physics Letters 113, 222402, (2018).
5. Hanbicki, A. et al. Applied Physics Letters 82, 4092-4094, (2003).
6. Jiang, X. et al. Physical Review Letters 94, 056601, (2005).
7. Awschalom, D. D. & Flatté, M. E. Nature physics 3, 153-159, (2007).
8. Hirohata, A. et al. Journal of Magnetism and Magnetic Materials 509, 166711, (2020).
9. Chuang, P. et al. Nature Nanotechnology 10, 35-39, (2015).
10. Dankert, A. & Dash, S. P. Nature Communications 8, 16093, (2017).
11. Kohda, M. & Salis, G. Semicond. Sci. Technol. 32 073002 (2017)
12. Moh. Adhib Ulil Absor & Ishii, F. Phys. Rev. B 100, 115104 (2019).
13. Autieri, C, Barone, P, Sławińska, J, & Silvia Picozzi, S. Phys. Rev. Materials 3, 084416 (2019).
14. Fert, A. & Jaffres, H. Physical Review B 64, 184420, (2001).